

Dynamic discrete models for the granular matter formation process

A. Khapalov and S. Lapin
 Department of Mathematics
 Pullman, WA 99163, USA
 email: khapala@math.wsu.edu

Abstract

In this paper we introduce 1- D and 2- D discrete models for the *dynamic* granular matter formation process in the form of a system of difference equations. This approach allows us to differentiate between the influx of the rolling layer coming down from different directions to the corner points of the standing layer. Such points are difficult to adequately describe by means of pde's and their straightforward numerical approximations, typically "ignoring" the system's behavior on the sets of zero measure. However, these points are critical for understanding the dynamic formation process when the standing layer is created by the moving front of the rolling matter or when the latter is filling a cavity and/or stops rolling. The existence of distributed (infinite dimensional) limit solutions to our discrete models as the size of mesh tends to zero is also discussed. We illustrate our findings by numerical examples which use our model as a direct algorithm.

1. Introduction.

1.1. Discussion of prior work in the field. In the last two decades there has been a substantial interest among physicists and applied mathematicians to mathematical models, both dynamic and static, describing the process of formation of granular matter. The motion patterns of granular materials are quite different from the behavior of classical phases such as solid continua, gases or fluids, see the discussion in this respect, e.g., in de Gennes [11]-[12], Haderer and Kuttler [13] and the references there in. Essentially, the formation of granular materials is viewed as the growth of so-called "standing" layer (whose height at point x at time t we further denote by $u(x, t) \geq 0$) due to the influx of a rolling layer (with the height $v(x, t) \geq 0$), which rolls down the slope of the standing layer under the gravity, see, e.g., Mehta et al [14], de Gennes [12] and the references there in. This process can be quite different for different materials (e.g., sand, snow, mud) due to the difference in their properties. In this paper we focus on the case when the granular material is a dry sand or similar matter, in which case we do *not* deal with such phenomena like mud slides or avalanches over the rock surface of the same fixed slope.

In Bouchaud et al [3]-[4] and Boutreux et al [6]-[6] the following 1- D model was suggested for the *local* process of granular matter formation:

$$v_t = sv_x - \gamma(\alpha - |u_x|)v, \quad (1.1)$$

$$u_t = \gamma(\alpha - |u_x|)v \quad \text{in } Q_T, \quad (1.2)$$

where $s > 0$ is to be the *constant* speed of the grains in the rolling layer when the standing layer slope is below its critical value α , and $\gamma > 0$ is a parameter. The choice of $s > 0$ means that

the rolling motion is directed to the left. The height of the standing layer at point x is to grow proportionally to the thickness of the rolling layer at this point. The height of the rolling layer grows proportionally to its slope minus the contribution to the standing layer.

Model (1.1)-(1.2) can be viewed as a “minimal empiric” model of the granular pile formation process and it captured its essential features. However, it leaves open a number of questions and concerns. In particular, it assumes that the speed of grains in the rolling layer does not depend on the slope of the standing layer. This model is also invalid when this slope changes sign. No stochastic effects or inertia are taken into account. These and some other problems were mentioned, e.g., in [13].

Several subsequent papers were aimed at the attempts to address the above concerns. In [11] it was suggested to add a diffusion term Du_{xx} with small D to take into account possible random effects, and to add “mathematical smoothness” into model (1.1)-(1.2). In [13] the following modifications of the above model were proposed:

$$v_t = \beta(vu_x)_x - \gamma(\alpha - |u_x|)v + f, \quad (1.3)$$

$$u_t = \gamma(\alpha - |u_x|)v, \quad (1.4)$$

$$u(x, 0) = u_o(x) \geq 0, \quad v(x, 0) = v_o(x) \geq 0, \quad |u_{ox}| \leq \alpha,$$

where f describes a possible external source of the granular matter. The first term on the right in (1.3) reflects the intention of the authors to make sure that the flow of the rolling layer follows the gradient of the standing layer.

The above models do not discuss the question of conservation of granular matter. Let us note that the above-cited models (both the original one and its modifications) were introduced in a rather empiric fashion. In this paper we intend to put more emphasis on the physical and mathematical justification of modeling ideas at hand.

In interesting papers Amadori and Shen [1]-[2] the existence of a global solution to system (1.3)-(1.4) with $f = 0$ was shown for small initial datum under the additional assumptions that the slope of the standing layer does not change sign and that it has an infinite length. These assumptions convert (1.3)-(1.4) into a qualitatively different Cauchy problem for 2x2 hyperbolic system of balance laws. But they also make the resulting model not quite realistic physically.

Other related publications. In Prigozhin [15] (see also [16] and the references therein) a variational approach to the granular matter formation problem was proposed in the form of a model consisting of a single equation for the standing layer, while the height of the rolling layer is to be viewed as a “selectable” parameter. It was shown that this model is equivalent to an evolutionary quasi-variational inequality. The existence and uniqueness results were established for the case of “no steep” slopes.

Several interesting explicit mathematical results were obtained in Cannarsa and Cardaliaguet et al [7], Cannarsa et al [8]-[9] for the *static version* of the aforementioned model in [15].

1.2. Motivation, main goals and layout of the paper. Our motivation for this paper is twofold.

Model (1.3)-(1.4) is well-recognized in the literature. However, recent computational experiments in Colombo et al [10] revealed certain irregularities in its behavior in some “non-standard” situations (such as when the standing layer forms a cavity, see Example 2.1 below). It was noticed in [10] that the mathematics of the aforementioned model equations allows the level of the granular matter to exceed its initial maximum at the subsequent moments of time. This phenomenon – labeled by the authors of [10] as “geysers” – seems to contradict the main underlying physical idea that the rolling matter should flow downward. Respectively, [10] proposed a new very different model for

the granular flow in the form of Cauchy problem for 3x3 system of balance laws. *In this paper* our goal is to try to offer a different modification of the original flow model (1.3)-(1.4). To this end, we investigate analytically which part of equations (1.3)-(1.4) is responsible for generation of “geysers” and then modify this part (namely, by omitting the 2nd order term in (1.3)).

The 2nd motivation point is that it seems that model (1.3)-(1.4) is not intended for the description of the behavior of the granular formation process near the corners of the standing layer, that is, at the points where the function describing it is not differentiable. More precisely, we focus here on: (a) the behavior of granular matter near the points where the standing layer meets its foundation and its slope is critical (i.e., *how the slope propagates horizontally?*) and (b) the process of filling cavities formed by the standing layer with critical slopes. *In this paper* we intend to overcome this challenge by proposing models in the form of *difference equations*, and show that, as the mesh size tends to zero, the respective discrete solutions converge to some limit distributed function (along some subsequences, in general). Our discrete models are linked to respective pde models under some regularity assumptions, which, in particular, exclude the aforementioned corner points.

The paper is organized as follows. In Section 2 we prove (by simple analytical means) that the maximum value of the total height of the granular matter in the 1-*D* model (1.3)-(1.4) may exceed its initial value at some later time. We show that this phenomenon is linked to the curvature of the surface of the standing layer and does *not* depend on the thickness of the rolling layer, nor on the thickness of the standing layer (see also Remark 2.1 below). The size of such emerging “geysers” can be substantial and cannot be viewed as just a minor effect of local diffusion, which was the reason in [11] to introduce the 2-nd order term $\beta v u_{xx}$ into the 1-st equation of model (1.3)-(1.4). We show that, if we drop the term $\beta v u_{xx}$ in (1.3), the aforementioned violation of the law of gravity will not occur. It appears that in the context of (1.3)-(1.4) the presence of this 2-nd order term $\beta v u_{xx}$ principally changes the “mathematical nature” of the problem at hand, because it becomes the senior order term in (1.3). Respectively, one cannot expect its contribution to be always “small”.

In Section 3 we show that the 2-nd equation in the 1-*D* model (1.3)-(1.4) may generate certain problems with the expected “physical accuracy” when the standing layer has corners. To address this issue, in *Section 4*, we introduce a 1-*D discrete* model for the dynamic granular matter formation described by the system of *difference equations*, i.e., instead of the usual partial differential equations. This approach seems to be novel to this field. Its main idea is that it will allow one to deal with the process at hand at the discretized level and, hence, to quantitatively distinguish between the amounts of the rolling matter coming down from the left and from the right to the *corner* points of the standing layer. These “points of lack of differentiability” are typical in the dynamic models when the standing layer is constantly re-created by the moving front of the rolling matter.

Let us elaborate a little further on the benefits of this approach over the traditional pde approach in the context of this particular physical phenomenon. Clearly, the function representing the height of the standing layer becomes non-differentiable at the corner points of the standing layer. The traditional pde approach (to modeling) usually “neglects” the behavior of the process at hand at such “isolated non-differentiable” points (e.g., making use of the concept of generalized non-differentiable solutions). However, in the case of granular flow, the corners of standing layer (e.g., at the foundation of a sand pile) appear to be of major significance and cannot be overlooked just as “unimportant isolated single points”. A possible way out here is the aforementioned difference equations approach.

We illustrate the advantages of our approach by computational experiments in Section 7, which directly use the respective difference equations of Section 4 as a computational algorithm. In particular, they show that the respective model (4.1)-(4.4) works well for any slopes, regardless of their length, sign, steepness and thickness.

In Section 5 we discuss the properties of model (4.1)-(4.4), which are used in Section 6 to prove the existence of its distributed limit solution by passing to the limit as the mesh size tends to zero. In Section 8 we extend our 1- D model to the case of two dimensions. Formal limits of our discrete models to those in the form of pde's, and their connection to existing models, are also discussed.

2. Diffusion term and the lack of compliance with the law of gravity in model (1.3)-(1.4). In this section we will re-visit the phenomenon of “geysers” in model (1.3)-(1.4), discovered in [10] solely by numerical means. Our goal here is to investigate it by means of formal analysis, which, in turn, will provide us with an idea what can be done to modify model equations (1.3)-(1.4) to avoid this phenomenon.

Suppose that, initially, the granular matter was located strictly inside of $(0, 1)$ and that $T > 0$ is small enough to ensure that during the flow process it would remain within $(0, 1)$. Thus, instead of (1.3)-(1.4) we will further deal with its homogeneous version in a bounded space domain:

$$v_t = \beta(vu_x)_x - \gamma(\alpha - |u_x|)v, \quad (2.1)$$

$$u_t = \gamma(\alpha - |u_x|)v, \quad (x, t) \in Q_T = (0, 1) \times (0, T), \quad (2.2)$$

$$u(x, 0) = u_o(x) \geq 0, \quad v(x, 0) = v_o(x) \geq 0, \quad |u_{ox}(x)| \leq \alpha, \quad x \in [0, 1],$$

$$u(x, t)|_{x=0,1} = 0, \quad v(x, t)|_{x=0,1} = 0, \quad t \in (0, T).$$

We formally assume below in our analysis that the functions $u, u_t, u_x, u_{xx}, v, v_t, v_x$ exist and are continuous in \bar{Q}_T and that there is no external source in model (1.3)-(1.4), i.e., $f = 0$.

Lack of compliance with the law of gravity in model (1.3)-(1.4)/(2.1)-(2.2). Suppose that, initially, the maximum value for $(u_o(x) + v_o(x))$ is reached at point $x_o, 0 < x_o < 1, u_o(x_o) + v_o(x_o) > 0$. Hence, $v_{ox} + u_{ox} = 0$, or $v_{ox} = -u_{ox}$, and $(v_o + u_o)_{xx} \leq 0$ at x_o . In turn, (2.1) yields that

$$(u + v)_t = -\beta u_{ox}^2 + \beta v_o u_{oxx} \text{ at } (x_o, 0). \quad (2.3)$$

Now note that the expression on the right in (2.3) *can* be positive when the term u_{oxx} is positive at $x = x_o$. In this case, the time-derivative of the height of granular matter $(u + v)_t|_{(x_o, t)}$ will be positive at and immediately after $t = 0$, and thus it will *have to increase* after $t = 0$ to exceed its maximum initial value $(u_o(x_o) + v_o(x_o))$. In other words, model (2.1)-(2.2) allows the rolling matter to roll upward, “defying” the gravity law.

Example 2.1: Geyser in a cavity. This example is a version of the situation investigated in [10] numerically. Suppose $u_o(x)$ has a cavity near the maximum point x_o of $u_o(x) + v_o(x)$ as shown in Fig. 1.

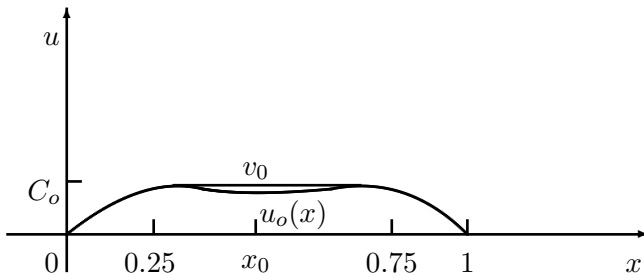


Figure 1 : “Geyser situation” in a cavity.

It is assumed that the maximum value C_o of the function $u_o(x) + v_o(x), x \in [0, 1]$ is reached *everywhere* between $x = 0.25$ and 0.75 with the rolling layer to be filling the cavity (e.g. sand “pushed/dropped” into a cavity). Then:

$$u_o(x) + v_o(x) = C_o, \quad v_o(x) = -u_o(x) + C_o, \quad x \in [0.25, 0.75].$$

We assume that $u_o(x)$ is strictly convex at x_o and $u_o(x_o)$ is the point of local minimum for $u_o(x)$, i.e., $u_{oxx}(x_o) > 0$. Hence, $v_o(x)$ is strictly concave at x_o , and $v_o(x_o)$ is the point of local maximum for $v_o(x)$. Respectively

$$v_{ox} = u_{ox} = 0, \quad (v_o + u_o)_{xx} = 0 \text{ at } x_o.$$

Therefore, in (2.3):

$$(u + v)_t = \beta v_o u_{oxx} > 0 \text{ at } x = x_o, t = 0. \quad (2.3)^*$$

Hence, the value of $(v(x, t) + u(x, t))$ will increase as t increases at x_o from its initial highest point, i.e., generating some sort of a “geyser” near this point.

Example 2.2: Geyser created by a ledge. In this example we take only *slightly more* than the right half of the cavity to form a “ledge” on the slope of the standing layer as shown on Figure 2. The same argument applies to show that one has a geyser at x_o .

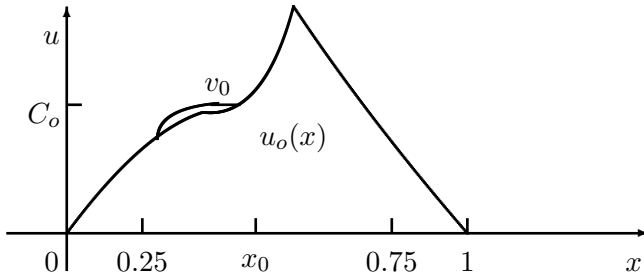


Figure 2 : Geyser situation in a “half – cavity”.

Remark 2.1: On “thin” and “thick” rolling slopes. We emphasize here that, due to (2.3), the above situation does not depend on the thickness of the rolling layer relative to the standing layer. It rather depends on the shape (curvature) of the *surface of the standing layer*. In particular, in the above counterexamples the depth of the cavity can be as “thin” as one wishes on the surface of the standing layer of an arbitrary height, which implies that the respective rolling layer can relatively be as “shallow ” as one wishes.

Modification of equation (1.3)/(2.1). We established in the above that the diffusion term $\beta v u_{xx}$ in model (1.3)-(1.4)/(2.1)-(2.2) can overpower the underlying law of gravity. This questions the accuracy of this model, at least in some situations. If this term is *dropped*, we will have the following model:

$$v_t = \beta v_x u_x - \gamma(\alpha - |u_x|)v, \quad (2.4)$$

$$u_t = \gamma(\alpha - |u_x|)v \quad \text{in } Q_T = (0, 1) \times (0, T), \quad (2.5)$$

$$u(x, 0) = u_o(x) \geq 0, \quad v(x, 0) = v_o(x) \geq 0, \quad |u_{ox}| \leq \alpha \quad x \in [0, 1],$$

$$u(x, t)|_{x=0,1} = 0, \quad v(x, t)|_{x=0,1} = 0 \quad t \in (0, T).$$

Let us show that model (2.4)-(2.5) fully complies with the law of gravity. The physical interpretation of equation (2.4) is straightforward. Let, say, $u_x > 0$, $u_x v_x > 0$ at some (x_o, t_o) as shown here:

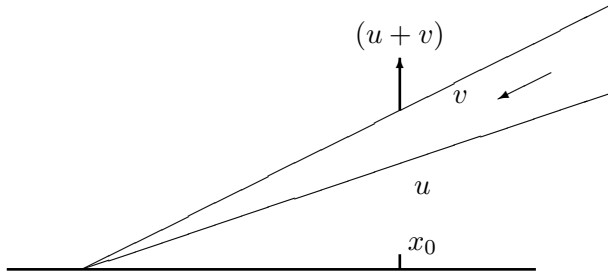


Figure 3 : $u_x, u_x v_x > 0$ at (x_0, t_0) .

On Fig. 3 the standing layer is rising at x_0 at time t_0 , and *relative to it*, the rolling layer is rising as well. Hence, the granular matter in the latter rolls down (to the left) and this *will* increase the value of $(u + v)$ at this point, as confirmed by (2.4), rewritten as follows:

$$(v + u) |_{(x_0, t)} = (v + u) |_{(x_0, t_0)} + \int_{t_0}^t v_x(x_0, \tau) u_x(x_0, \tau) d\tau.$$

The next picture illustrates the case when $u_x > 0$, $u_x v_x < 0$ at some (x_0, t_0) .

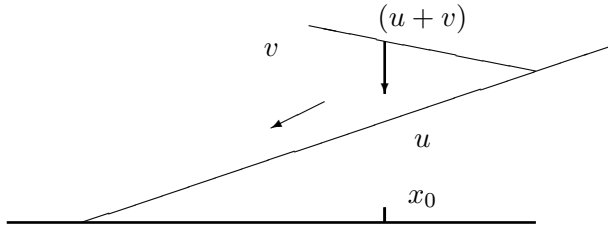


Figure 4 : $u_x > 0$, $u_x v_x < 0$ at (x_0, t_0) .

Proposition 2.1: Compliance of model (2.4)-(2.5) with the law of gravity. *The maximum value of $u(x, t) + v(x, t)$ for the model (2.4)-(2.5) is attained at $t = t_0$.*

Proof. The proof is quite simple and makes use of the idea of the classical proof of the maximum principle for the linear 1-d heat equation.

We argue by contradiction and consider only the nontrivial case: $v + u \not\equiv 0$ in Q_T . Let the function $(u(x, t) + v(x, t))$ attain its global maximum in $[0, 1] \times [0, T]$, which is *strictly greater* than $\max_{x \in [0, 1]} (v_0(x) + u_0(x))$, at some point $x_0 \in (0, 1)$ (recall here that $(v + u) |_{x=0, 1} = 0$) at a positive moment time. Then, by continuity, the same is true for the function $(v^*(x, t) + u^*(x, t))$, where $v^* = e^{-kt}v$, $u^* = e^{-kt}u$ and $k > 0$ is a “small” positive parameter. Now, let the just-mentioned (*non-zero*) global maximum for the function $(v^*(x, t) + u^*(x, t))$ be attained at (x^*, t^*) , where $x^* \in (0, 1), t^* > 0$. If so, we should have

$$e^{-kt}(v + u)_x = (v^* + u^*)_x = 0, \quad (v^* + u^*)_t \geq 0 \text{ at } (x^*, t^*)$$

(we use the left-hand side time-derivative if $t^* = T$). However, due to (2.4):

$$(u^* + v^*)_t = -ke^{-kt}(v + u) - \beta e^{-kt}v_x^2 < 0 \text{ at } (x^*, t^*).$$

Hence, we arrived at contradiction. End of proof.

Remark 2.2: Comparison of Proposition 2.1 with the classical maximum principle for parabolic pde’s. There is a resemblance between Proposition 2.1 and the classical maximum

principle for the *linear* 1-*d* heat equation, which states that the extreme values of the temperature within a spatial domain are attained either at the initial moment or on the boundary of this domain. This principle reflects the main underlying physical law of the heat transfer. However, the heat equation is a *scalar linear* pde, while Proposition 2.1 deals with a 2-*D nonlinear system* of pde's. Thus, it makes it a novelty how one can setup a “maximum principle” for system like (2.4)-(2.5). Note that Proposition 2.1 does *not* deal with the separate maximum values of functions u and v .

3. Behavior of model (1.3)-(1.4)/(2.1)-(2.2) near the corners in the standing layer created by the critical slope(s). Our goal here is to explain the reasons for our further modifications of this model as suggested below.

Equation (2.2)/(1.4) does not allow the standing layer to grow at the points where the slope is critical, i.e., when $|u_x| = \alpha$ and, thus, $u_t = 0$. Consider, e.g., the case when the base of the standing layer is extending due to influx of the rolling matter, as illustrated by Figures 5 and 6:

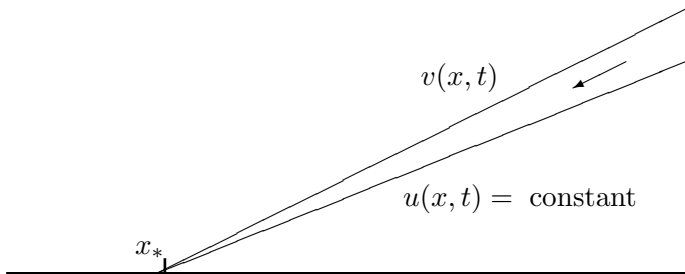


Figure 5 : The case of critical slope.

Let assume that the slope of the standing layer u on Fig. 5 is critical ($u_x = \alpha$) on the right of the corner point x_* , i.e., where it meets the horizontal base. Then, due to (1.4)/(2.2),

$$u_t(x, t) = 0, \quad u(x, t) = u(x, 0) = u_o(x), \quad t > 0, \quad x > x_*, \quad (3.1)$$

and, thus, all the material in the rolling layer will have to roll to the left of this corner point, leaving the standing layer unchanged (see also Remark 3.1 below). However, the physical expectations here are associated with a build-up of the standing layer *on both sides of x_** , e.g., as shown on Fig. 6:

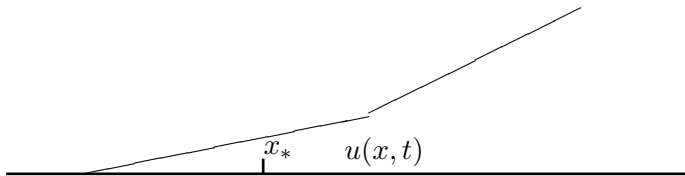


Figure 6 : Expected evolution of the standing layer from Fig. 5.

Fig. 6 is not compatible with (1.4)/(2.2). Thus, this equation is not accurate in this case, i.e., when there is a transition from the critical slope to a lesser one.

Remark 3.1. In Figs. 5 the standing layer has a *nondifferentiable* slope at x_* . Hence, model (1.3)-(1.4)/(2.1)-(2.2) cannot be applied in the classical sense. If, to deal with it (say, numerically), we assume that

$$u_x(x_*, 0) = \frac{1}{2}(0 + \alpha),$$

i.e., take the average of slopes from the right and from the left, this will only result in the growth of $u(x, t)$ at x_* due to equation (1.4)/(2.2) (this growth at a single point does not make “physical” sense). However, on the right of x_* the slope will remain critical and hence still cannot grow into a physically expected formation as on Figure 6.

Cavity. Similar to the above, in the case when the standing layer has a cavity as on Figure 7(b) below with both slopes converging to the same point to be critical, equations (1.4)/(2.2) will not allow these slopes to grow when there is a rolling matter on either of them. We propose a way out in this situation in the next section (see also numerical examples 7.1-2 in Section 7).

“Abrupt halt and full conversion” of the rolling matter. If there is no inertia, then, when the rolling matter arrives to the *lowest* corner point of the cavity, it should immediately stop and instantaneously be *fully* converted into the standing layer at this point. This phenomenon is impossible to describe by means of pde’s like in (1.3)-(1.4) (one may consider, e.g., δ -functions for that).

4. 1-D difference equations model. The discussion in Section 3 indicates that the situations when the standing layer has corners create serious problems for modeling by means of pde’s. Mathematically, these situations are associated with the spatial points where the 1-st spatial derivative u_x does not exist. In our opinion, this justifies attempts to try to look for different types of model equations which do not deal with differentiable (both in the classical and generalized sense) functions.

Our approach below, to address the just-outlined issue, deals with an attempt to *convert the above-discussed pde model* (2.4)-(2.5) into an associated *discrete model*, which would intrinsically allow us to use one-sided derivatives to distinguish between the amounts of the rolling matter coming down from the left and from the right to the corner points of the standing layer (or rolling down away from them). In the process of construction of this model, we intend to focus on its physical interpretation and to discuss all possible cases of mutual orientations of slopes at hand.

Let us split the interval $[0, 1]$ into n equal segments of size $\Delta_n x$, and the time-interval $[0, T]$ into m equal segments of size $\Delta_m t$.

Remark 4.1. In what follows, the size of time-step will be allowed to change to smaller values before we reached the moment T . Nonetheless, for simplicity of notations we will use the same m below. The space-step remains constant for the given system. (One, of course, can select a different mesh strategy.)

The solution of the approximate system is represented by the collection of values denoted by $\{u_{i,j}^{(n,m)}, v_{i,j}^{(n,m)}, i = 0, \dots, n, j = 0, \dots\}$. These values define the *piecewise linear* approximate solution, denoted for the standing layer by $u^{(n,m)}(x, t)$ and for the rolling layer by $v^{(n,m)}(x, t)$, $x \in [0, 1], t \in [0, T]$, to the granular matter formation process at hand for the respective nodes $\{(x_i, t_j), i = 1, \dots, n, j = 0, \dots\}$. For example,

$$u_{0,0}^{(n,m)} = u^{(n,m)}(0, 0), \quad u_{1,1}^{(n,m)} = u^{(n,m)}(\Delta_n x, \Delta_m t), \quad \text{and so forth.}$$

The physical idea behind the propagation of rolling matter, exploited in this paper, is that it can move *only downward* due to the force of gravity. Therefore, the changes happening to the combined rolling and standing layers at point $x_i = i\Delta_n x$ are to be the result only of the *matter* (a) *arriving down to it from the adjacent rising slope(s)* and/or (b) *leaving down along the adjacent falling slope(s)*.

Remark 4.2. The above means that, in what follows, we do not take into account other possible motions of the granular matter such as, e.g., of stochastic nature or due to inertia, etc.

Note that, unlike models (2.1)-(2.2) and (2.4)-(2.5), in the case of difference equations approach we will deal with *the left- and right-hands sides derivatives* of our piecewise linear approximate

functions $u^{(n,m)}(x, t)$. Three principal cases are possible near the point x_i (case (7(a)) has also its symmetric double about the vertical line passing through x_i):

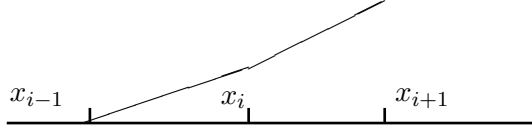


Figure 7(a) : Slope is rising to the right of x_i only. Both slopes can be zero.

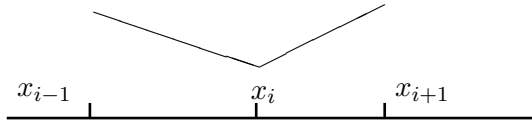


Figure 7(b) : A “cavity” near x_i with slopes rising on both sides of x_i .

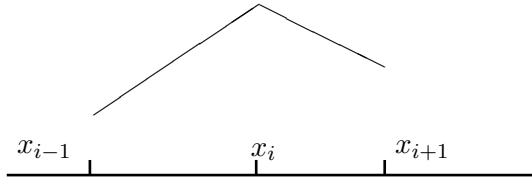


Figure 7(c) : A “vertex/peak” at x_i with slopes falling on both sides of x_i .

To approximate the time derivative at point (x_i, t_j) , we use the standard forward approximation:

$$u_t \approx \frac{u^{(n,m)}(x_i, t_{j+1}) - u^{(n,m)}(x_i, t_j)}{\Delta_m t}.$$

To approximate the spatial derivative at point (x_i, t_j) , we use respectively the derivatives of $u^{(n,m)}(x, t)$:

$$u_{x+}^{(n,m)}(x_i, t_j) = \frac{u^{(n,m)}(x_{i+1}, t_j) - u^{(n,m)}(x_i, t_j)}{+\Delta_n x},$$

$$u_{x-}^{(n,m)}(x_i, t_j) = \frac{u^{(n,m)}(x_{i-1}, t_j) - u^{(n,m)}(x_i, t_j)}{-\Delta_n x}.$$

Our equations (4.1)-(4.2) below are derived based on the discussions around Figures 3-7(a-c).

Difference equations for the standing layer. In this case we assume that the increase of the height of the standing layer is defined by the slope(s) of the standing layer *below* the given grid point as the one(s) determining:

- how much of the rolling matter *available at this point will stay there*
- and *how much of it will roll down*, namely:

$$\begin{aligned}
& u^{(n,m)}(x_i, t_{j+1}) = u^{(n,m)}(x_i, t_j) \\
& + \gamma \Delta_m t \left\{ \begin{array}{ll}
(\alpha - |u_{x-}^{(n,m)}(x_i, t_j)|)v^{(n,m)}(x_i, t_j) & \text{for } u_{x+}^{(n,m)}(x_i, t_j) \geq 0, \quad u_{x-}^{(n,m)}(x_i, t_j) > 0 \\
(\alpha - |u_{x+}^{(n,m)}(x_i, t_j)|)v^{(n,m)}(x_i, t_j) & \text{for } u_{x-}^{(n,m)}(x_i, t_j) \leq 0, \quad u_{x+}^{(n,m)}(x_i, t_j) < 0 \\
\frac{1}{\gamma \Delta_m t} v^{(n,m)}(x_i, t_j) & \text{for } u_{x+}^{(n,m)}(x_i, t_j) \geq 0, \quad u_{x-}^{(n,m)}(x_i, t_j) = 0, \\
\frac{1}{\gamma \Delta_m t} v^{(n,m)}(x_i, t_j) & \text{for } u_{x-}^{(n,m)}(x_i, t_j) \leq 0, \quad u_{x+}^{(n,m)}(x_i, t_j) = 0, \\
\frac{1}{\gamma \Delta_m t} v^{(n,m)}(x_i, t_j) & \text{for } u_{x+}^{(n,m)}(x_i, t_j) \geq 0, \quad u_{x-}^{(n,m)}(x_i, t_j) \leq 0, \\
r_{i,j,-} (\alpha - |u_{x-}^{(n,m)}(x_i, t_j)|)v^{(n,m)}(x_i, t_j) & \\
+ r_{i,j,+} (\alpha - |u_{x+}^{(n,m)}(x_i, t_j)|)v^{(n,m)}(x_i, t_j) & \text{for } u_{x+}^{(n,m)}(x_i, t_j) < 0, \quad u_{x-}^{(n,m)}(x_i, t_j) > 0.
\end{array} \right. \tag{4.1}
\end{aligned}$$

Note that formulas (4.1) will not immediately increase the slopes beyond the critical value both to the left and to the right of point x_i for Fig. 7(a) and/or its symmetric counterpart – if $\Delta_m t$ is sufficiently small (see Remark 4.1). When the lower slope is zero or like on Fig. 7(b), there is no lower slope for rolling down from x_i , and therefore all the rolling matter at this point becomes an addition to the standing layer at this point. (Let us remind the reader that in our model we do not take inertia into consideration.) In the case of Fig. 7(c) we assume that the rolling matter will all roll down along the steepest slope as defined by the following choice of splitting coefficients $r_{i,j,\pm}$:

$$r_{i,j,-} = \begin{cases} 1 & \text{if } |u_{x-}^{(n,m)}(x_i, t_j)| > |u_{x+}^{(n,m)}(x_i, t_j)| \\ 0 & \text{if } |u_{x-}^{(n,m)}(x_i, t_j)| < |u_{x+}^{(n,m)}(x_i, t_j)| \\ \frac{1}{2} & \text{if } |u_{x-}^{(n,m)}(x_i, t_j)| = |u_{x+}^{(n,m)}(x_i, t_j)| \end{cases}$$

while $r_{i,j,+}$ is defined symmetrically. This strategy will ensure, in particular, that either slope, on the left and on the right of x_i , will not exceed the critical value. Namely, if at least one of the aforementioned slopes is critical, then the standing layer will not increase at x_i .

Denote

$$v_*^{(n,m)}(x_i, t_j) = v^{(n,m)}(x_i, t_j) - \left(u^{(n,m)}(x_i, t_{j+1}) - u^{(n,m)}(x_i, t_j) \right),$$

where (and in (4.1)) the term in the large parenthesis describes the increase of the height of the standing layer during the time-interval (t_j, t_{j+1}) due to the contribution from the rolling layer available at time t_j . Thus, $v_*^{(n,m)}(x_i, t_j)$ describes the part of the rolling layer at x_i which will leave this point rolling down a respective slope (unless we have the situation as on Fig. 7(b)) after $t = t_j$. In other words, we assume that the contribution of the rolling layer to the standing layer on the interval $[t_j, t_{j+1}]$ occurs at time t_j . Respectively, in equations (4.2) for the rolling layer, we will use the following notations:

$$v_{*x+}^{(n,m)}(x_i, t_j) = \frac{v_*^{(n,m)}(x_{i+1}, t_j) - v_*^{(n,m)}(x_i, t_j)}{+\Delta_n x},$$

$$v_{*x-}^{(n,m)}(x_i, t_j) = \frac{v_*^{(n,m)}(x_{i-1}, t_j) - v_*^{(n,m)}(x_i, t_j)}{-\Delta_n x}.$$

Difference equations for the rolling layer:

$$v^{(n,m)}(x_i, t_{j+1}) = v_*^{(n,m)}(x_i, t_j) + \Delta_m t \beta \mathbf{F}, \tag{4.2}$$

where (see also Fig. 8 and explanations to it):

$$\mathbf{F} = r_{i+1,j+1,-} u_{x+}^{(n,m)}(x_i, t_{j+1}) v_{*x+}^{(n,m)}(x_i, t_j)$$

for the case like on Fig. 7(a) when $u_{x_+}^{(n,m)}(x_i, t_{j+1}) \geq 0$, $u_{x_-}^{(n,m)}(x_i, t_{j+1}) \geq 0$;

$$\mathbf{F} = r_{i-1,j+1,+} u_{x_-}^{(n,m)}(x_i, t_{j+1}) v_{*x_-}^{(n,m)}(x_i, t_j)$$

for $u_{x_-}^{(n,m)}(x_i, t_{j+1}) \leq 0$, $u_{x_+}^{(n,m)}(x_i, t_{j+1}) \leq 0$;

$$\mathbf{F} = r_{i+1,j+1,-} u_{x_+}^{(n,m)}(x_i, t_{j+1}) v_{*x_+}^{(n,m)}(x_i, t_{j+1}) + r_{i-1,j+1,+} u_{x_-}^{(n,m)}(x_i, t_{j+1}) v_{*x_-}^{(n,m)}(x_i, t_{j+1})$$

for the case like on Fig. 7(b);

$$\mathbf{F} = -\frac{1}{\Delta_m t \beta} v_*^{(n,m)}(x_i, t_j)$$

for Fig. 7(c) when $u_{x_+}^{(n,m)}(x_i, t_{j+1}) \leq 0$, $u_{x_-}^{(n,m)}(x_i, t_{j+1}) \geq 0$, i.e., when there is no influx of rolling matter (all the prior matter will leave the peak).

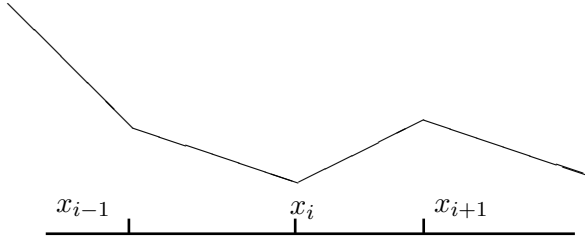


Figure 8 : A “cavity” near x_i with slopes rising on both sides of x_i .
At x_{i+1} we have an “above peak”, no “peak” at x_{i-1} .

Figure 8 illustrates the idea of the choice of splitting coefficients in (4.2). To describe the forthcoming changes in the height of the rolling layer at point x_i , we rely only on the slopes *above* the respective grid point, i.e., where the rolling matter is coming from.

The initial and boundary conditions for equations (4.1)-(4.2) are defined similar to those in (2.1)-(2.2):

$$u^{(n,m)}(0, t_j) = u^{(n,m)}(1, t_j) = 0, \quad j = 0, 1, \dots,$$

$$u^{(n,m)}(x_i, 0) = u_0(x_i) \geq 0, \quad v^{(n,m)}(x_i, 0) = v_0(x_i, 0) \geq 0, \quad i = 0, \dots, n, \quad (4.3)$$

$$|u_{x_{\pm}}^{(n,m)}(x_i, 0)| \leq \alpha, \quad i = 1, \dots, n-1. \quad (4.4)$$

5. Properties of solutions to the difference equations. Let us remind the reader that we assumed in the above that we can regulate the size of time step in (4.1)-(4.2) to preserve conditions (4.3) and (4.4) (see Remark 4.1).

Property 5.1: Compliance of model (4.1)-(4.4) with the law of gravity. Similar to Proposition 2.1, the following inequality holds *with proper selection of the time-steps* in (4.1)-(4.2):

$$\begin{aligned} & \max_{i=1, \dots, n; j=1, \dots} \{u^{(n,m)}(x_i, t_j) + v^{(n,m)}(x_i, t_j)\} \\ & \leq \max_{i=1, \dots, n} \{u^{(n,m)}(x_i, 0) + v^{(n,m)}(x_i, 0)\} \end{aligned} \quad (5.1)$$

Indeed, it follows from (4.2) (see the last line) that in order to have

$$u^{(n,m)}(x_{i_0}, \Delta_m t) + v^{(n,m)}(x_{i_0}, \Delta_m t) \geq u^{(n,m)}(x_{i_0}, 0) + v^{(n,m)}(x_{i_0}, 0)$$

for some $\Delta_m t$, one of the slopes $u_{x_{\pm}}^{(n,m)}(x_i, \Delta_m t)$ should rise away from the point x_{i_0} and the respective slope $v_{*x_{\pm}}^{(n,m)}(x_{i_0}, 0)$ should be of the same sign too. This is impossible, since

$$u^{(n,m)}(x_{i_0}, \Delta_m t) + v_*^{(n,m)}(x_{i_0}, 0) = u^{(n,m)}(x_{i_0}, 0) + v^{(n,m)}(x_{i_0}, 0)$$

and the right-hand side is the top vertex for the combined sum of layers at $t = 0$.

Hence, a possible inequality contradicting to (5.1) at time t may arise only at some $x_i \neq x_{i_0}$ with an initially strictly lower sum of two layers. Therefore, due to the fact that these are finitely many, we can select, if necessary from now on a new, smaller step size $\Delta_{m^*} t$ which will guarantee (5.1) at time $t = \Delta_{m^*} t$ with the equality at such spatial node point(s).

Property 5.2: The critical slope restriction. At time $t = 0$ we have necessary conditions for that as given by (4.4). The explanations after (4.1) show that this restriction cannot be violated immediately. If, however, $u_{x_+}^{(n,m)}(x_i, t_j)$ or $u_{x_-}^{(n,m)}(x_i, t_j)$ will exceed the critical value at some moment t_j , we are to return to the prior time-layer and to select a new smaller value for the time-step which will not result in the violation of the critical slope requirement. This process can go on till $u_x^{(n,m)}(x_i, t_j)$ had reached the critical slope everywhere and thus we have reached the saturated (static) solution.

Property 5.3: Nonnegativity of solutions. Equations (4.1) imply that in order for some of $u^{(n,m)}(x_i, t_{j+1})$'s become negative, some of $v^{(n,m)}(x_i, t_j)$ must become negative first. Let, e.g., at some point (x_i, t_j) (t_j can be zero) the value of $v^{(n,m)}(x_i, t_j)$ becomes zero for the first time (for suitably adjusted $\Delta_m t$), while $u^{(n,m)}(x_i, t_j) \geq 0$. In this case the sum of two layers at time t_{j+1} will not decrease at x_i . Indeed, in this case the slopes $v_{*x_{\pm}}^{(n,m)}$ on either side of x_i are either equal to zero or are rising *away* from it at time t_j . Hence, the last term on the right in (4.2) can be nonzero only if $u_{x_{\pm}}^{(n,m)}$ are also rising away from x_i at time t_{j+1} , because (4.2) takes into account only the standing layer slope(s) which lie above the respective grid point. Hence, the last term on the right of (4.2) is non-negative in our case and therefore the sum of two layers cannot decrease at x_i .

Next, since $v_*^{(n,m)}(x_i, t_j) = v^{(n,m)}(x_i, t_j) = 0$, (4.1) means that

$$u^{(n,m)}(x_i, t_{j+1}) = u^{(n,m)}(x_i, t_j) \geq 0 \text{ at } x_i.$$

Thus, for the aforementioned sum of two layers not to decrease at time t_j , the value of $v^{(n,m)}(x_i, t_{j+1})$ must remain nonnegative.

Property 5.4: Preservation of growth of $u^{(n,m)}(x_i, t_j)$ in time. This follows immediately from (5.2) under Properties 5.2-3.

6. Existence of a distributed solution to the dynamic granular formation problem as a limit solution to model (4.1)-(4.4). Note that the properties 5.1-4 mean that the sequence of functions $\{u^{(n,m)}(x, t)\}_{\Delta_n x, \Delta_m t}$ is uniformly bounded in $H_0^{1,0}(Q_T) = \{\phi \mid \phi, \phi_x \in L^2(Q_T), \phi|_{x=0,1} = 0\}$, and is equicontinuous and uniformly bounded in $C(\bar{Q}_T)$. Therefore, the Arzela-Ascoli Theorem yields that it contains a uniformly converging subsequence. Without loss of generality, we can say that

$$u^{(n,m)}(x, t) \rightarrow u_*(x, t)$$

as $\Delta_n x, \Delta_m t \rightarrow 0+$ in $C(\bar{Q}_T)$ and weakly in $H^{1,0}(Q_T)$. This limit function satisfies all the Properties 5.1, 5.3-4 in the continuous form. In turn, the slope restriction is satisfied in the ‘‘generalized’’ sense: the graph of function $u_*(x, t)$ in x for any t lies within the cone with center at point $(x, u_*(x, t)) \in R^2$ and slopes ± 1 , while $u_*(x, t)$ is non-decreasing in time for any x .

Respectively, the sequence of functions $\{v^{(n,m)}(x, t)\}_{\Delta_n x, \Delta_m t}$ is uniformly bounded in $L^\infty(Q_T)$, and thus also in $L^2(Q_T)$. Therefore, without loss of generality, we can say that

$$v^{(n,m)}(x, t) \rightarrow v_*(x, t) \text{ as } \Delta_n x, \Delta_m t \rightarrow 0+ \text{ weakly in } L^2(Q_T).$$

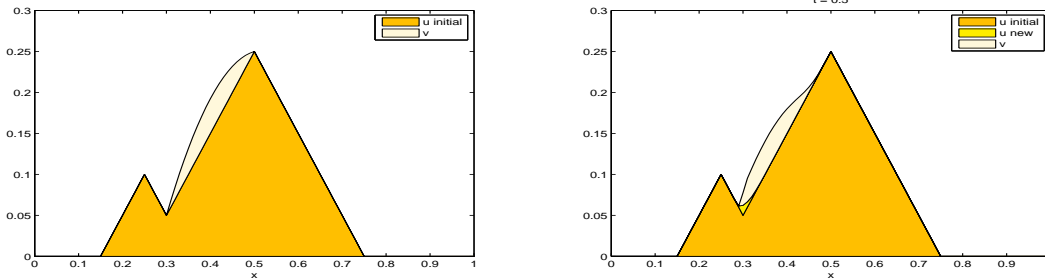


Figure 9: Example 7.1: The case when the initial standing layer has a cavity at $x = 0.3$. Initial configuration (left) and configuration at $t=0.5$ (right).

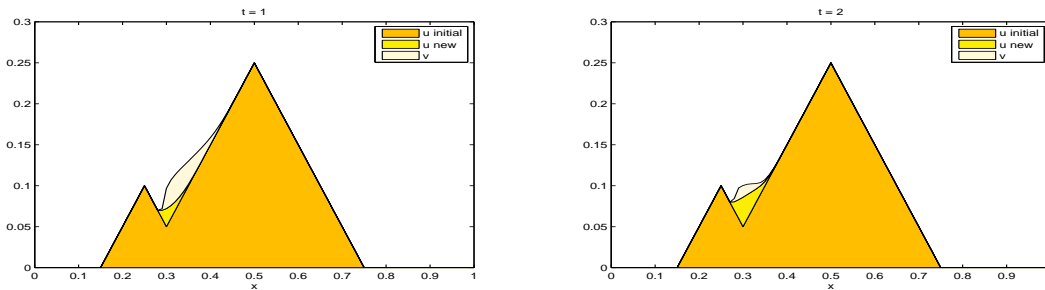


Figure 10: Example 7.1: Configuration at $t=1.0$ (left) and $t=2.0$ (right).

Connection to pde modeling. The difference equations (4.1)-(4.4) can be viewed as approximation of pde model (2.4)-(2.5) at points (x, t) where u and v are continuously differentiable and $u_x \neq 0$.

7. Model (4.1)-(4.4), computational strategy and examples. In model (2.1)-(2.2) the second-order diffusion term is "symmetric", while the first-order convective term is "directional". For small values of β the diffusion is "empirically small" compared to convection, i.e., in some situations the model exhibit strong propagation behavior for the most of the domain. In this case approximation of the convective terms by central difference leads to nonphysical oscillations [17]. On the other hand the proposed difference model (4.1)-(4.4) takes care of the aforementioned phenomena. The finite differences in the model are adaptively directional, taking into account the direction of propagation at each space step, thus allowing simulate accurately various configurations of standing and rolling matter. In the two examples 7.1 and 7.2 illustrated respectively by Figures 9-11 and 12-14 we employ directly the difference equations (4.1)-(4.4) as a numerical algorithm, assuming uniform finite difference mesh in space and time and $\alpha = 1, \gamma = 1$.

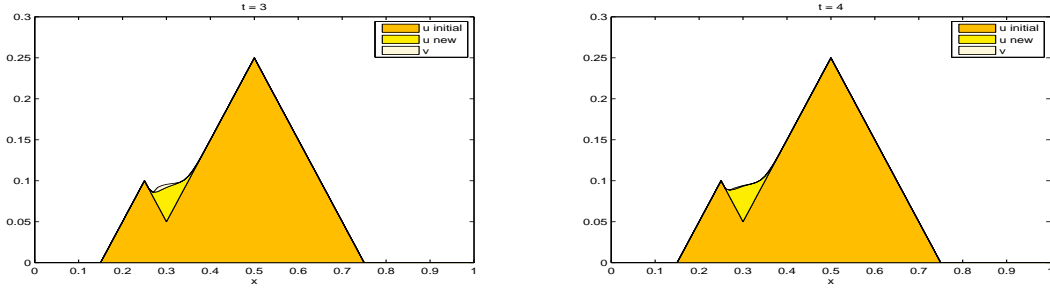


Figure 11: Example 7.1: Configuration at $t=3.0$ (left) and $t=4.0$ (right).

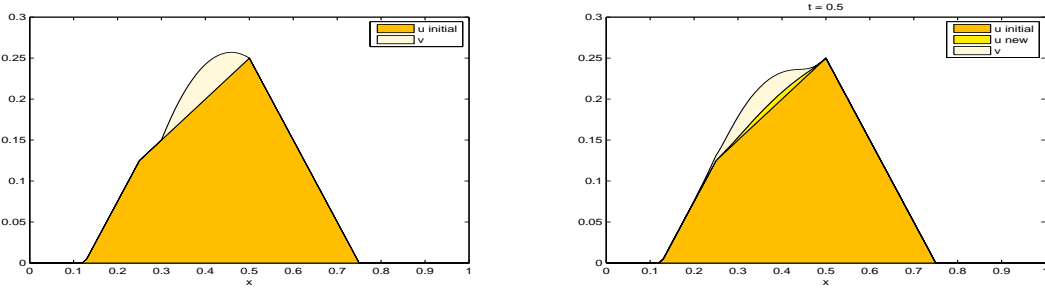


Figure 12: Example 7.2 : The case when the left slope of the initial standing layer changes from non-critical value to critical. Initial configuration (left) and $t=0.5$ (right).

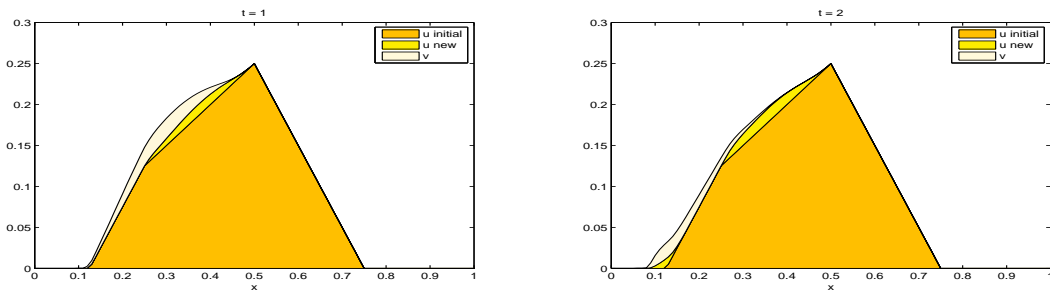


Figure 13: Example 7.2: Configuration at $t=1.0$ (left) and $t=2.0$ (right).

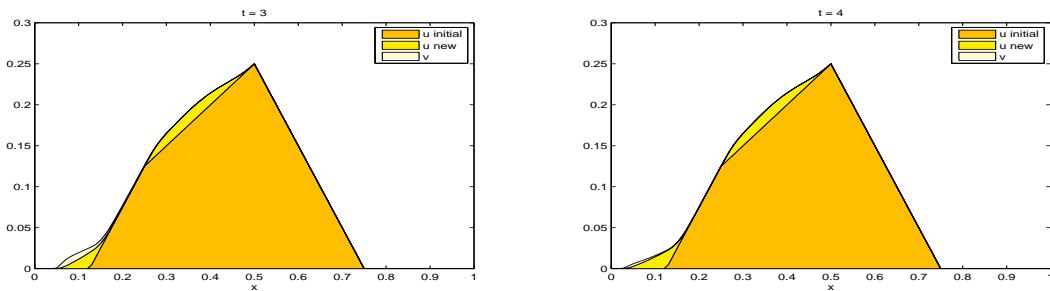


Figure 14: Example 7.2: Configuration at $t=3.0$ (left) and $t=4.0$ (right).

All the models in the above (i.e., (1.1)-(1.2), (1.3)-(1.4)/(2.1)-(2.2), (2.4)-(2.5),(4.1)-(4.4)) do *not* explicitly address the question of conservation of the total granular matter. Our numerical results indicate that, given the initial standing and rolling layers, this issue is linked to the value of coefficient β in the equations for the rolling layer.

8. 2-D granular formation difference equations. We will now assume that u and v are functions of two spatial variables x and y : $u = u(x, y, t), v = v(x, y, t)$. In the 1-D model (4.1)-(4.4) we dealt with the flow of granular matter propagating along the x -axis only. In the 2-D model we will respectively deal with the flows propagating between the nodes of the chosen mesh. We intend to use the standard rectangular-shaped mesh on the xy -plane and will propose a 2-D discrete model which will describe the propagation of the granular matter between the respective adjacent nodes parallel to the x - and y -axes. As usual, one has certain freedom to chose the interpolation method for the spatial points which are not the nodes.

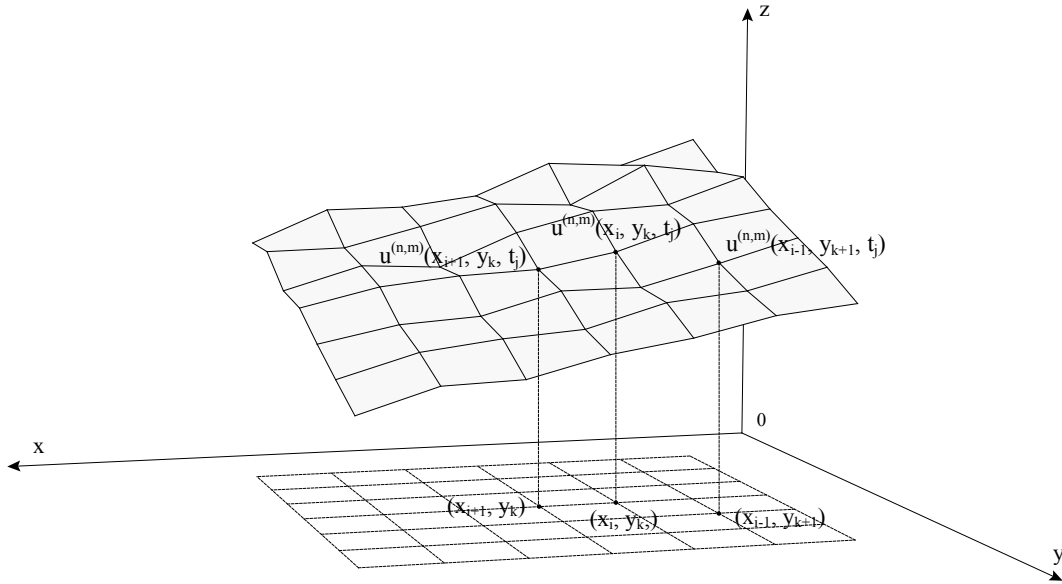


Figure 15: Illustration of possible reconstruction of the standing layer in the 2-D model.

We will preserve the notations of Section 4 wherever it will be possible. Let $(x, y) \in [0, 1] \times [0, 1] = \Omega$. Split Ω into $n \times n$ equal squares (one can consider rectangles as well) of size $\Delta_n x = \Delta_n y$, and the time-interval $[0, T]$ into m equal segments of size $\Delta_m t$. The solution of the approximate system is represented by the collection of values denoted by $\{u_{i,k,j}^{(n,m)}, v_{i,k,j}^{(n,m)}; i, k = 0, \dots, n, j = 0, \dots, m\}$. These values will define, depending on the chosen strategy for interpolation, an approximate solution in Ω , denoted for the standing layer by $u^{(n,m)}(x, y, t)$ and for the rolling layer by $v^{(n,m)}(x, y, t), (x, y) \in [0, 1] \times [0, 1], t \in [0, T]$, see Fig 15 for illustration.

To approximate the time derivative at point (x_i, y_k, t_j) , we use the same standard forward approximation as in Section 4. The same we will do for the x - and y -spatial derivative, e.g.,

$$u_{x_{\pm}}^{(n,m)}(x_i, y_k, t_j) = \frac{u^{(n,m)}(x_{i\pm 1}, y_k, t_j) - u^{(n,m)}(x_i, y_k, t_j)}{\Delta_n x},$$

$$u_{y\pm}^{(n,m)}(x_i, y_k, t_j) = \frac{u^{(n,m)}(x_i, y_{k\pm 1}, t_j) - u^{(n,m)}(x_i, y_k, t_j)}{\Delta_n y}.$$

Difference equations for the standing layer. Its value will be determined by the *sum* of movements of the granular matter along the x - and y -axes:

$$u^{(n,m)}(x_i, y_k, t_{j+1}) = u_{(x)}^{(n,m)}(x_i, y_k, t_{j+1}) + u_{(y)}^{(n,m)}(x_i, y_k, t_{j+1}), \quad (8.1)$$

where $u_{(x)}^{(n,m)}(x_i, y_k, t_{j+1})$ represents the propagation of this matter along the x -axis and is calculated for each $y_k, k = 1, \dots, n-1$ exactly as in (4.1) for the respectively modified notations in the list of variables: (x_i, t_j) in (4.1) should be replaced by (x_i, y_k, t_j) . However, in this case each of the nodes (x_i, y_k) deals with four directions, i.e., along both the x - and y -axes, instead of two as in the 1- D case. In each term on the right of (8.1) (compare to (4.1)) we will need to use a respective splitting coefficient. For example, if at instant t_j at the node (x_i, y_k) in the negative direction along the x -axis we have the steepest slope and the slopes in other three directions are strictly smaller, then the respective splitting coefficient $r_{i,k,j,x-} = 1$. If it is one of two steepest slopes, $r_{i,k,j,x-} = 1/2$, and so forth.

Denote

$$v_*^{(n,m)}(x_i, y_k, t_j) = v^{(n,m)}(x_i, y_k, t_j) - \left(u^{(n,m)}(x_i, y_k, t_{j+1}) - u^{(n,m)}(x_i, y_k, t_j) \right),$$

where the term in the large parenthesis describes the increase of the height of the standing layer during the time-interval (t_j, t_{j+1}) due to the contribution from the rolling layer available at time t_j (compare to (4.1)-(4.4)). Thus, $v_*^{(n,m)}(x_i, y_k, t_j)$ describes the part of the rolling layer at x_i which will leave this point rolling down a respective slope. In other words, as in the 1- D case, we assume that the contribution of the rolling layer to the standing layer on the interval $[t_j, t_{j+1}]$ occurs at time t_j . Denote:

$$v_{*x\pm}^{(n,m)}(x_i, y_k, t_j) = \frac{v_*^{(n,m)}(x_{i\pm 1}, y_k, t_j) - v_*^{(n,m)}(x_i, t_j)}{+\Delta_n x},$$

$$v_{*y\pm}^{(n,m)}(x_i, y_k, t_j) = \frac{v_*^{(n,m)}(x_i, y_{k\pm 1}, t_j) - v_*^{(n,m)}(x_i, y_k, t_j)}{+\Delta_n x}.$$

The difference equations for the rolling layer. In the above notations we obtain the following system of equations:

$$v^{(n,m)}(x_i, y_k, t_{j+1}) = v_*^{(n,m)}(x_i, y_k, t_j) + \Delta_m t \beta (\mathbb{F}_x + \mathbb{F}_y) \quad (8.2)$$

where \mathbb{F}_x represents the motion of the rolling layer along the x -axis and \mathbb{F}_y along the y -axis with the following ‘‘correction’’. Namely, the respective terms in (8.2) will have the splitting coefficients like $r_{i,k,j,x\pm}$ in (8.1) in the above.

The initial and boundary conditions for equations (8.1)-(8.2) are defined similar to those in (4.1)-(4.2):

$$u^{(n,m)}(x_i, 0, t_j) = u^{(n,m)}(x_k, 1, t_j) = u^{(n,m)}(0, y_k, t_j) = u^{(n,m)}(1, y_k, t_j) = 0, \quad j = 1, \dots,$$

$$u^{(n,m)}(x_i, y_k, 0) = u_0(x_i, y_k,) \geq 0, \quad v^{(n,m)}(x_i, y_k, 0) = v_0(x_i, y_k, 0) \geq 0, \quad i, k = 0, \dots, n, \quad (8.3)$$

$$\max\{ |u_{x\pm}^{(n,m)}(x_i, y_k, 0)|, |u_{y\pm}^{(n,m)}(x_i, y_k, 0)| \} \leq \alpha, \quad i, k = 1, \dots, n-1. \quad (8.4)$$

The convergence results of Section 6 can be extended to model (8.1)-(8.4) in a similar way.

Connection to pde modeling. The difference equations (8.1)-(8.4) can be viewed as approximation of the following pde model at the points (x, y, t) where u and v are continuously differentiable and $u_x \neq 0 \neq u_y$ (compare to (2.4)-(2.5)):

$$v_t = -u_t + \beta \nabla u \cdot \nabla v, \quad (8.5)$$

$$u_t = \gamma(\alpha - |\nabla u|), \quad (8.6)$$

$$u(x, 0) = u_o(x) \geq 0, \quad v(x, 0) = v_o(x) \geq 0, \quad \max\{|u_{ox}|, |u_{oy}|\} \leq \alpha \quad x \in [0, 1],$$

$$u(x, t) |_{\partial\Omega} = 0, \quad v(x, t) |_{\partial\Omega} = 0 \quad t \in (0, T).$$

Note that our discrete model (8.1)-(8.2) is intended to restrict the maximum of directional derivatives of u by the critical value along the directions parallel to the x - and y -axes (with further use of suitable interpolation elsewhere). When u is differentiable, this maximum is equal to $|\nabla u|$. Note that it is not the case when we deal with non-differentiable points of the standing layer such as the vertices of cones. In this case, one can use the following equation in place of (8.6):

$$u_t = \gamma(\alpha - \max_{s \in R^2} \{|D_s u|\}),$$

where $D_s u$ stands for the directional derivative of u in the direction s .

Concluding remark on the discrete nature of models (4.1)-(4.4), (8.1)-(8.4). One can view our discrete models (4.1)-(4.4) and (8.1)-(8.4) as “unnecessarily complex”. Let us argue, however, that in order to calculate a solution of any highly nonlinear granular matter formation model, one will have to use *some* discrete model. Thus, the crux of the problem here is the strategy on how to choose one, i.e., not just any abstract discretization, but a discretization which will preserve the physical properties of the process at hand. Models (4.1)-(4.4) and (8.1)-(8.4) are aimed exactly at this issue (see also an opening paragraph in Section 7 on the numerical aspects of various approximation methods).

References

- [1] D. Amadori and Wen Shen, Mathematical Aspects of a Model for Granular Flow, In “IMA Volumes in Mathematics and its Applications”, vol. 153, “Nonlinear Conservation Laws and Applications”, pp. 169–180. Springer, 2011. Editors: A. Bressan, G-Q. Chen, M. Lewicka and D. Wang.
- [2] D. Amadori and Wen Shen, Global Existence of Large BV Solutions in a Model of Granular Flow. *Comm PDE*, 34 (2009), n0. 7-9, 1003-1040.
- [3] J.-P. Bouchaud, M.E. Gates, J.R. Prakash, S.F. Edwards, A model for dynamics of sandpile surfaces, *J. Phys. I France*, 4 (1994), pp. 1383-1410.
- [4] J.-P. Bouchaud, M.E. Gates, J.R. Prakash, S.F. Edwards, Hysteresis and metastability in a continuum sandpile model, *Phys. Rev. Lett.*, 74 (1995), 1982-1985.
- [5] T. Boutreux and P.-G. Gennes, Surface flow of granular mixture, I. General principles and minimal model, *J. Phys. I France*, 6 (1996), 1295-1304.
- [6] T. Boutreux and P.-G. Gennes, Étatement d’une marche de sable: le le problème du Sinai, *C.R. Acad. Sci. Paris*, 325 (1997), Sér. B, 85-89.

- [7] P. Cannarsa and P. Cardaliaguet, Representation of equilibrium solutions to the table problem for growing sand plies, *J. Eur. Math. Soc.*, **6** (2004), pp. 435-464.
- [8] P. Cannarsa, P. Cardaliaguet, G. Crasta, and E. Georgieri, A boundary value problem for PDE model in mass transfer theory: Representation of solutions an applications, *Calc. Var.* , **24(4)** (2005), pp. 431-457 (DOI 10.1007/s00526-005-0328-7).
- [9] P. Cannarsa, P. Cardaliaguet, and C. Sinestrari, On a differential model for growing sand piles with non-regular sources, *CPDE*.
- [10] R.M. Colombo, Gr. Guerra, and F. Monti, Modeling the dynamics of granular matter, *IMA J Appl Math* (2012) 77(2): 140-156.
- [11] P.-G. de Gennes, Dynamique superficielle d'un matériau granulaire, *C.R. Acad. Sci. Paris*, **321** [Iib] (1995), 85-89
- [12] P.-G. de Gennes, Granular matter: a tentative view, *Rev. Mod. Phys.*, **71** (1999), 374382.
- [13] K.P. Haderler and Christina Kuttler, Dynamic models for granular matter, *Granular Matter*, **2** (1999).
- [14] A. Mehta, R. Needs, S. Dattagupta, The Langevin dynamics of vibrated powders, *J. Stat. Phys.*, **68** (1992), 1131-1141.
- [15] L. Prigozhin, Variational model of sand pile growth, *Euro. Jnl. of Applied Mathematics*, **7** (1996), pp. 225-235.
- [16] L. Prigozhin and B. Prigozhin and Zaltsman, On the approximation of the dynamics of sandpile surfaces, *Phys. Rev E*, **63** (2001) 041505.
- [17] J.W. Thomas, Numerical partial differential equations: Finite difference methods, *Springer-Verlag*, (1995)